Fetal MRI: State of the Art and New Insights

Lucia Manganaro[1], Marco Gennarini[1], Ilaria Balba[2], Giulia Cundari[1], Alessandra Maiuro[3], Angelica Cupertino[1], Nicola Galea[1], Valentina Miceli[1], Silvia Capuani[3], Carlo Catalano[1]

[1]Department of Radiological, Oncological and Pathological Sciences, Umberto I Hospital, Sapienza University of Rome, Italy
[2]Siemens Healthcare S.r.l., dARE, Milan, Italy
[3]CNR ISC c/o Physics Department, Sapienza University of Rome, Italy

Introduction

Fetal magnetic resonance imaging (fMRI) is a second-level diagnostic modality performed after morphological ultrasonography that offers crucial insights for fetal and placental assessment [1, 2]. It boasts numerous advantages, including safety, high-resolution tissue contrast, and the ability to surpass the limitations of ultrasound (US) examinations. fMRI indications encompass both the central nervous system and fetal body assessments. Common indications pertaining to the central nervous system include ventriculomegaly, midline malformations, posterior fossa malformations, supratentorial parenchymal lesions or destruction, ischemic hemorrhagic lesions, infective diseases, facial malformations (e.g., cleft lip/palate), and neural tube defects [3]. In the evaluation of the fetal body, typical indications for fMRI include congenital diaphragmatic hernia, neck masses, fetal airway obstruction, congenital pulmonary malformations, meconium peritonitis, sacrococcygeal teratoma, abdominal/pelvic masses, and lower urinary tract obstruction [4].

Recent technological advances have led to the development of new sequences and new software capable of providing and interpreting qualitative and quantitative data for investigating different pathological conditions and fetal malformations [5]. Furthermore, new studies show safety in exposing fetuses[1] to high magnetic fields such as those from 3T MRI [6]. This review aims to describe the latest news in fMRI. It places particular emphasis on the new fMRI sequences, specifically diffusion-weighted imaging (DWI) techniques, including intravoxel incoherent motion (IVIM); on the transition from 1.5T to 3T magnets; and on the possibilities that artificial intelligence (AI) and radiomics offer for fMRI.

Advanced clinical perspectives: State of the art in fetal MRI

MRI has numerous indications concerning the brain and fetal body, and the study of the placenta [1, 7].

Due to the scarcity of evidence in the literature and the objective difficulties of execution to date, it is not possible to include areas of the musculoskeletal structures, particularly the limbs and the osteo-cartilaginous component of the forming spine.

Studies of the fetal central nervous system account for 80% of fMRI requests. The most frequent indications according to international guidelines include ventriculomegaly, hydrocephalus, midline abnormalities (Fig. 1), TORCH infections, ischemic hemorrhagic lesions, cortical malformations, and posterior cranial fossa abnormalities [8–10].

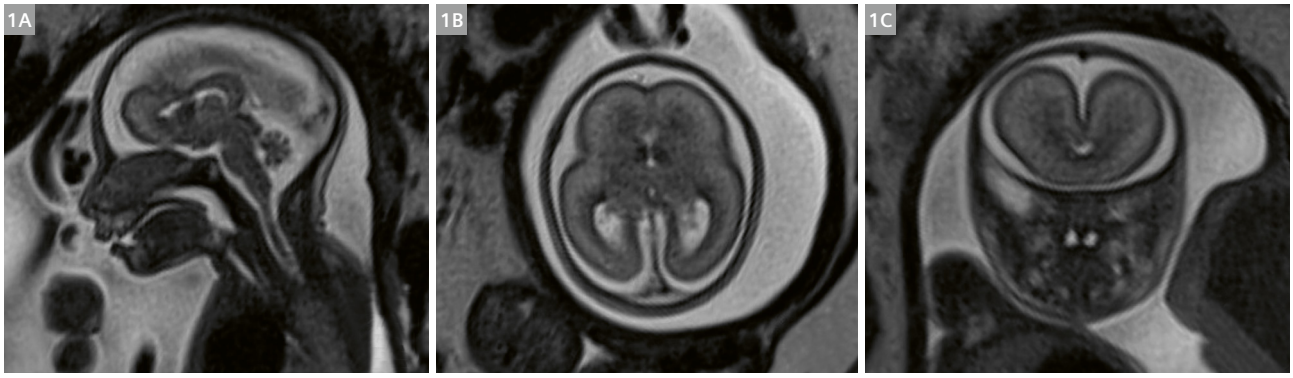

1 T2-weighted images acquired on a 3T scanner in sagittal **(1A)**, axial **(1B)**, and coronal **(1C)** planes in a syndromic fetus with dysgenesis of the corpus callosum and lobar holoprosencephaly.

[1]*Siemens Healthineers disclaimer: MR scanning has not been established as safe for imaging fetuses and infants less than two years of age. The responsible physician must evaluate the benefits of the MR examination compared to those of other imaging procedures. This disclaimer does not represent the opinion of the authors.*

Fetal body indications concern neck, thoracic, and abdominal structures. This is despite the fact that – excluding congenital diaphragmatic hernia and neck masses – indications for abdominal examination are not well defined.

The most studied cervical lesions are teratoma, cystic lymphatic malformations, and hemangioma [11].

The indication for further diagnostic investigation with MRI for the fetal thorax is justified by the fact that lung anatomy and morphology are clearly recognized in T2-weighted sequences. In addition, DWI acquisitions make it possible to study the degree of lung maturity, given that the apparent diffusion coefficient (ADC) value increases with advancing gestational age (GA).

The examination is proposed in fetuses with congenital chest mass, congenital pulmonary airway malformation, and congenital diaphragmatic hernia. This is because these conditions are associated with pulmonary hypoplasia (Figs. 2 and 3).

In our clinical practice, most examinations are generally performed at 20 to 23 gestational weeks to confirm and/or exclude a malformation after a second-level morphologic US examination. In addition, examinations are now increasingly being requested in the third trimester to choose delivery modality and subsequent treatment of the fetus in cases of malformative, metabolic, or placental pathologies.

Important indications are represented by placental insertion abnormalities and placenta accreta spectrum (PAS) disorders. Therefore, a correct diagnosis and an accurate choice of delivery timing is essential. In our clinical practice, and according to scientific literature, the most frequent indications concerning the fetal brain are TORCH infections, midline abnormalities, ventriculomegaly, and posterior cranial fossa pathology. As for indications concerning the fetal body, the most frequent are congenital diaphragmatic hernia; neck masses; abnormalities of the urinary, gastrointestinal, and pulmonary tracts; complex malformations; and growth restriction.

Application of a proper study protocol includes the use of T2-weighted, T1-weighted with and without fat saturation, TrueFISP, and DWI sequences. T2-weighted sequences allow morphological visualization of normal fetal anatomical structures or possible abnormalities. T1-weighted sequences with and without fat suppression enable better characterization of the content of the different structures, detecting the presence of adipose, hemorrhagic, and proteinaceous components.

The use of DWI sequences allows recognition of hypercellular tissue formations, such as tumor formations, which result in more difficult movement of free water molecules and are represented by signal hyperintensity. In addition, diffusion sequences are particularly useful in the study of ischemic-hemorrhagic lesions, twin-to-twin transfusion syndrome, and the study of fetal kidneys in cases of suspected agenesis/ectopy.

Recently, we have also begun using advanced diffusion models such as IVIM, which allows us to discriminate diffusion perfusion. IVIM also makes it possible to

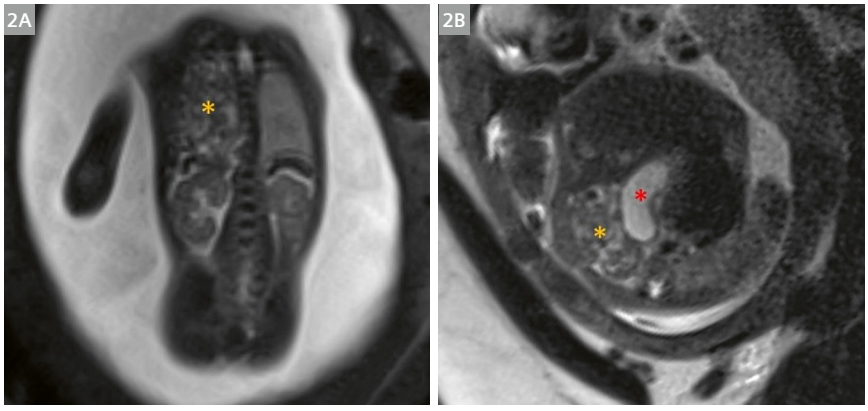

2 T2-weighted images acquired on a 3T scanner in coronal **(2A)** and axial **(2B)** planes in a fetus with congenital diaphragmatic hernia. Herniated intestinal loops (yellow *) and stomach (red *) in the chest.

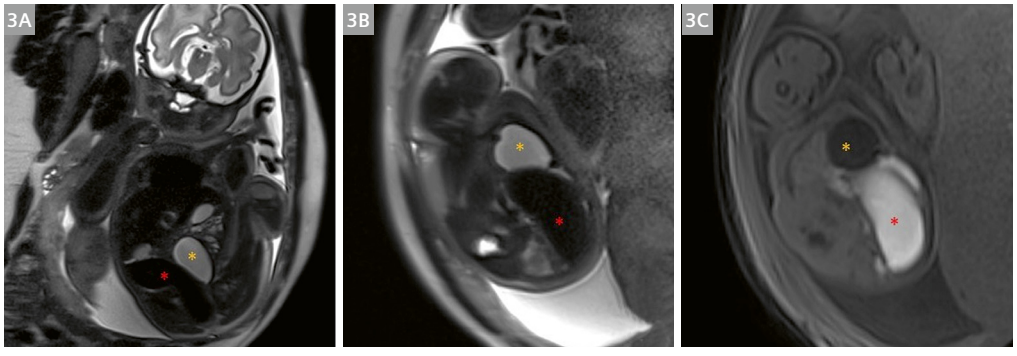

3 T2-weighted images acquired in coronal **(3A)** and axial **(3B)** planes, and T1-weighted fs image acquired in axial plane **(3C)** on a 3T scanner in a fetus with dilated intestinal loop. Dilated intestinal loop (red *) and bladder (yellow *).

assess – thanks to perfusion parameters, particularly f and D* – the microstructural tissue changes that occur in the fetal lungs and kidneys during gestation [12] and may help distinguish the various patterns of placental microvascularization in cases of small for gestational age (SGA) and fetal growth restriction (FGR).

When studying placental tissue, which is highly perfused, it is very important to also obtain separate estimations of perfusion and diffusion.

Perfusion measures blood circulation in the vascular bed per unit volume. It is an important marker of tissue viability and can be measured directly using intravascular contrast agents or metabolic tracers.

However, due to a lack of sufficient evidence in humans about the safety of contrast agents during pregnancy, tissue viability is often assessed using non-invasive techniques and indirect markers of tissue perfusion (such as Doppler US). In this context, the IVIM technique has been adapted to fMRI.

FGR is associated with several short- and long-term complications. It is defined as an estimated fetal weight that is less than the 10th percentile for GA by prenatal US evaluation.

In SGA and FGR, various degrees of structural abnormalities of the placental parenchyma, such as hypercellularity, tissue heterogeneity, and high fibrin deposition by fibroblasts, are responsible for the decrease in diffusion during the gestational period.

In prenatal clinical practice, US examination alone does not discriminate between SGA and FGR placentas because it does not allow for measuring perfusion in depth or microvascularization. IVIM, however, shows a significantly higher perfusion fraction f in normal placentas, lower in FGR placentas, and an intermediate value in SGA placentas [13].

Moreover, a significant positive correlation was found between f and body weight in FGR and SGA placentas, and a significant negative correlation was found between D and GA in the SGA and FGR group but not in the normal pregnancy group [13]. Therefore, f measured in the placenta can predict body weight.

IVIM can also be applied to the study of fetal body development. Some studies suggest that the progressive increase in renal and pulmonary blood flow characterizes normal pregnancy, resulting in an increase in overall tissue perfusion [12]. Therefore, perfusion fraction f in IVIM has the potential to investigate perfusion and diffusion qualities of the microstructural tissue changes that occur in renal and lung parenchyma during intrauterine life. These findings may be useful for distinguishing normal fetuses from pathological fetuses with intrauterine growth restriction.

The fetal brain is also much more perfused than the adult brain, so it could be investigated with the IVIM model. However, to achieve sufficient spatial resolution to study the fetal brain, the acquisition time of the IVIM protocol [14] may be too long. A recent study [15] shows that the fetal brain can be studied by quantifying ADC but renouncing the perfusion estimation: By normalizing DWI at different values of b data with DWI at a b-value of 50 s/mm^2, the perfusion bias in estimating ADC values is greatly reduced.

This proves that one of the main advantages of IVIM is the possibility to quantify not only the perfusion fraction but also the diffusion coefficient D without the bias due to the perfusion component present in the DWI signal obtained at low b-values. For this reason, the D parameter evaluated with the IVIM model is more sensitive to changes in tissue hypercellularity than the ADC parameter.

Transition to 3T

The recommendations from the Fetal Imaging Task Force of the European Society of Paediatric Radiology [16] regarding the preferred magnetic fields for various indications in fMRI are outlined as follows:

1. For neurological indications, particularly those involving the posterior cranial fossa, brain parenchymal lesions, and small median structures, it is preferable to use 3T MRI if available.
2. In cases involving fetal body indications, such as identifying herniated organs in diaphragmatic hernia cases, assessing smaller abdominal and pelvic organs, and evaluating cartilages, 3T MRI is preferred when accessible.
3. In instances of polyhydramnios, 1.5T MRI is favored. This is due to the more prominent shielding effects and resulting artifacts observed at 3T.
4. GA should not influence the choice of magnetic field strength.

The guidelines from the International Society of Ultrasound in Obstetrics and Gynecology, updated in 2023 [17], do not express a preference between 3T or 1.5T scanners. They acknowledge that 1.5T scanners can achieve satisfactory image resolution even at 18 months' GA, while also recognizing the higher resolution of images obtained by 3T scanners with a comparable energy deposition rate on tissues. However, for conditions like polyhydramnios, they recommend a 1.5T scanner, due to its reduced susceptibility to artifacts related to fluid waves [17].

Over the past few decades, 3T scanners have transitioned from being primarily used in research to becoming valuable clinical tools for fMRI [18]. The increased signal-to-noise ratio resulting from the higher field strength can be leveraged to accelerate acquisition, which is essential for compensating for sudden fetal movement or enhancing spatial resolution to achieve a more accurate depiction of the fetus.

The initial survey of fetal imaging practices in Europe, published in 2020, revealed that merely 30% of fMRI examinations are conducted at 3T. The reasons for this include the fact that not all centers have 3T magnets, as well as concerns regarding potential fetal harm and an uptick in artifacts.

Concerns regarding potential fetal harm were associated with the rise in specific absorption rate (SAR), the elevated noise produced by 3T magnets with the possible impact on the fetal auditory system, and the potential for causing intrauterine growth retardation [16]. However, there is currently no evidence suggesting that 3T MRI results in growth retardation or harms the auditory system [6, 19].

As magnetic field intensity increases, so does the release of radiofrequency energy, which raises SAR. The Food and Drug Administration (FDA) in the USA has established a threshold value of 4 W/kg for the maternal whole body [20]. Consequently, when transitioning from 1.5T to 3T, it is imperative to adjust the sequence parameters, as safety systems prevent exposure surpassing these threshold values [21].

The increase in field strength also leads to artifacts such as chemical shift, B1 inhomogeneity, and standing wave [22]. While these issues may be present at 1.5T, they become more pronounced and require attention at 3T. Dielectric artifacts pose a challenge in fetal imaging, manifesting as darker regions within the image due to the shorter wavelengths of radiofrequency waves compared to the scanned object [23]. This effect is accentuated when the abdominal diameters of patients exceed the radiofrequency wavelength (a common occurrence in pregnant women), particularly due to the dielectric properties of amniotic fluid [24].

Furthermore, variations in T1 and T2* relaxation times between different tissues depend on the magnetic field strength [22], posing a challenge in achieving the desired image contrast. Specifically, the T2* of the fetal placenta is significantly lower at 3T than 1.5T, potentially compromising the accurate evaluation of D and D* IVIM parameters. To address this limitation, DWI acquisitions should employ echo times substantially shorter than T2*.

Victoria et al. [25] compared 1.5T and 3T MRI in fetuses with matched GA and similar anomalies, assessing and scoring the resulting images. The evaluated anatomical structures were the intestine, liver, kidney, airway, cartilage, and spine. Scores for image evaluation ranged from 0 to 4, with 4 representing the highest image quality. The study revealed a general advantage of 3T imaging, which yielded higher scores than 1.5T imaging, with the best scores achieved using a TrueFISP sequence [25].

Regarding placental assessment, a recent study by Bourgioti et al. [26] involving 182 pregnant women demonstrated that the diagnostic efficacy of 1.5T and 3T MRI in evaluating PAS is largely comparable [26].

Fetal neuroimaging

Investigating the brain in small fetuses is one of the most difficult tasks in clinical imaging, primarily due to the unpredictable movements of the unborn child. This endeavor entails delineating small anatomical structures and discerning the transient layers of the developing cerebral hemispheres, which, due to the low contrast, poses significant challenges [27].

Nevertheless, 3T MRI scanners offer potential solutions to these challenges concerning contrast, as outlined in the preceding paragraphs. T2-weighted images, in particular, afford optimal contrast for delineating anatomical differences within the fetal brain, especially regarding water and lipid content in the mature brain. Furthermore, the heightened signal acquired through stronger gradients can be leveraged to enhance resolution and acceleration factors.

The swift imaging strategy used in fMRI is a beneficial approach that has already demonstrated efficacy in pediatric imaging. Turbo spin-echo sequences are particularly prone to motion artifacts, which can compromise the accurate diagnosis of brain abnormalities. In response to this challenge, Righini et al. [28] explored a shorter two-dimensional (2D) turbo spin-echo and fluid-attenuated inversion-recovery (FLAIR) sequence designed for investigating pediatric brains, capitalizing on the advantages offered by 3T scanners. The condensed protocol lasts only 52 seconds and is an intriguing option for fetal brain imaging with the aim of ascertaining whether the motion artifact is tolerable or requires exclusion.

It is widely recognized that 3T scanners present significant advantages in the field of neuroimaging, especially concerning fMRI, where assessing the fetal cerebral blood oxygenation status is crucial for identifying fetuses at risk of brain injury [29]. Central to this effort is the precise quantification of susceptibility in fetal cerebral vessels, a task accomplished through quantitative susceptibility mapping (QSM) facilitated by susceptibility-weighted imaging (SWI), a multi-echo gradient sequence known for its lengthiness and sensitivity to motion. However, emerging advancements in high-acceleration imaging technologies offer a promising pathway to achieving optimal outcomes with reduced scan time.

One such technology is wave-controlled aliasing in parallel imaging (Wave-CAIPI) SWI, which has been able to shorten brain scans from 5 to 2 minutes in adults [30].

This technique integrates two imaging methodologies, Wave and CAIPIRINHA, which involve oscillated gradients applied in both the slice and phase-encoding directions during readout, resulting in a corkscrew *k*-space trajectory. Additionally, parallel imaging incorporating coil sensitivity

knowledge helps mitigate undersampling artifacts and *g*-factor noise, thereby enhancing tolerance for high acceleration factors [31].

While this technology holds promise for fMRI, its application requires further exploration. The utility of Wave-CAIPI SWI extends beyond susceptibility quantification for QSM; it is also applicable to other neuro sequences, such as T1-weighted magnetization-prepared rapid gradient-echo (MPRAGE) and T2-weighted sampling perfection with application-optimized contrasts using different flip angle evolution (SPACE), enabling visualization of even smaller structures within a reasonable acquisition time [32].

Patient preparation and safety measures: Essential considerations

When conducting fMRI, ensuring the comfort of patients is crucial, as abdominal discomfort and patient movement can significantly affect the overall quality of the examination. It may be necessary to determine whether the patient can maintain the supine position for a certain amount of time; otherwise, adopting a lateral position could make the examination more comfortable. Once the patient is prepared, one or two 18-channel body matrix coils are employed in conjunction with the spine array coil. When conducting scans during pregnancy, utmost consideration must be given to both maternal and fetal safety. Radiofrequency exposure should be limited to prevent excessive heating, and normal mode settings for limiting SAR should be adopted. The lowest gradient modes available for each sequence are employed whenever feasible, and low SAR RF pulse types are used.

Guidelines from the International Society of Ultrasound in Obstetrics and Gynecology [17] suggest including at least T2-weighted sequences in three orthogonal planes of the fetal brain and body, and T1-weighted and gradient-echo (GRE) echo-planar imaging (EPI) sequences in one or two orthogonal planes, preferably frontal and sagittal [17]. In view of these guidelines, we propose the following 3T MRI protocol.

Optimizing fundamental protocols for 3T MRI scanning

The examination includes T1-weighted VIBE in the axial plane of the brain with and without fat suppression using the Dixon technique, as well as a T2 HASTE sequence in the axial, sagittal, and coronal planes of the brain.

Brain tissue T1 contrast is generally diminished at 3T compared to 1.5T [22]. Compensating for this loss of T1 contrast may necessitate a longer repetition times (TR) and the correction of the flip angle, thereby increasing acquisition time. Parallel imaging combined with VIBE allows for acquisitions during breath-hold, mitigating some fetal and maternal motion (Figs 4A, 4B).

Commonly used in fetal imaging, free-breathing single-shot turbo spin-echo (SS-TSE or HASTE) sequences facilitate the capture of entire volumes slice by slice [22] (Fig. 4C). However, unexpected fetal motion can compromise image quality, potentially requiring reacquisition. Depending on factors like body region and patient physiology, another unpredictable artifact is the dielectric artifact, or B1 inhomogeneity [23]. Pregnant individuals often have abdominal diameters exceeding ~30–50 cm, making the dielectric artifact difficult to avoid. Moreover, the presence of amniotic fluid can disrupt B1 homogeneity within the imaging field [23]. Techniques such as using saturation bands and adjusting flip angles help mitigate dark regions in images, but they may inadvertently increase RF power deposition, necessitating longer TR to stay within SAR

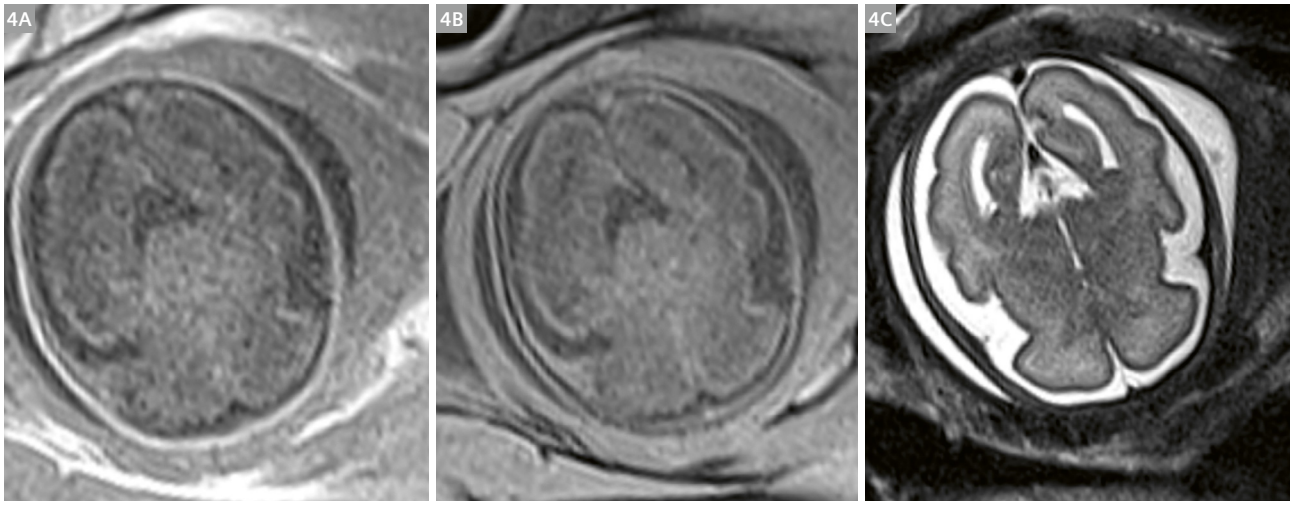

4 Transverse view of a 29-week-old fetus: **(4A)** T1-weighted in-phase acquisition, **(4B)** T1-weighted fat-saturated image, **(4C)** T2-weighted acquisition.

limits. This is the reason why employing a prescan B1 filter could be an option to adopt, since it can minimize signal discrepancies caused by dielectric resonances, especially at higher field strengths [33]. Depending on fetal positioning, relocating the shading artifact may be beneficial, particularly if the fetal brain is distant from the body array coil.

True fast imaging with steady state precession (True-FISP) provides high signal-to-noise ratio and T2/T1 image contrast, and it contributes to a more effective study of the fetal body. It employs a GRE sequence where the excited magnetization is maintained in the transverse plane using balanced gradient pulses [34]. It is advantageous for heart and vessel evaluation, due to bright-blood signal that contrasts with the dark-blood appearance in SS-FSE. Adjusting the offset frequency may be necessary to mitigate increased banding artifacts by relocating them outside the region of interest [35]. Different offsets lead to varying image contrasts due to the complex signal evolution within tissues. Modifying the frequency offset may also result in a different, possibly preferrable contrast (Fig. 5).

Over the last few years, fMRI has been considered an additional prenatal diagnostic tool that has significantly enhanced our understanding of and diagnostic accuracy in assessing placental and fetal abnormalities [36].

Thanks to advancements in DWI methodologies [37], and to the use of ADC maps [38, 39] and IVIM imaging protocols [36–42], it has become feasible to acquire quantitative data for assessing fetal microstructure and perfusion. These quantitative measures offer insights that supplement US examinations. The IVIM model uses DWI sequences at different diffusion weights (b-values), making it possible to separately quantify perfusion fraction f, which measures the perfusion fraction of water molecules perfused in microcapillaries with a D* rate and diffusion coefficient D. The DWI acquisitions are characterized by several b-values that are lower (less than 150s/mm^2) than in standard diffusion imaging in order to quantify perfusion parameters f and D*, in addition to D without the perfusion bias [41, 43] (Fig. 6). Generally, 10 b-values between 0 and 1000 are acquired with a total image acquisition time of about 4 minutes 30 seconds. This method does not involve substantial increases in SAR that would impair the implementation of the sequence, and offers excellent anatomic resolution.

Exploring fetal cardiac MRI

Fetal cardiac MRI (fCMR) is gaining importance in diagnosing congenital heart diseases (CHDs) in fetuses, especially when traditional US imaging faces limitations like poor acoustic windows due to factors such as maternal obesity, oligohydramnios, fetal lie, or calcified ribs [44, 45]. CHDs are the prevalent prenatal fetal abnormalities, with an incidence rate of 9 per 1000 births, making early detection and diagnosis essential. The most common CHD types in fetuses include atrial septal defects and coarctation of the aorta, but various other malformations can also occur [11].

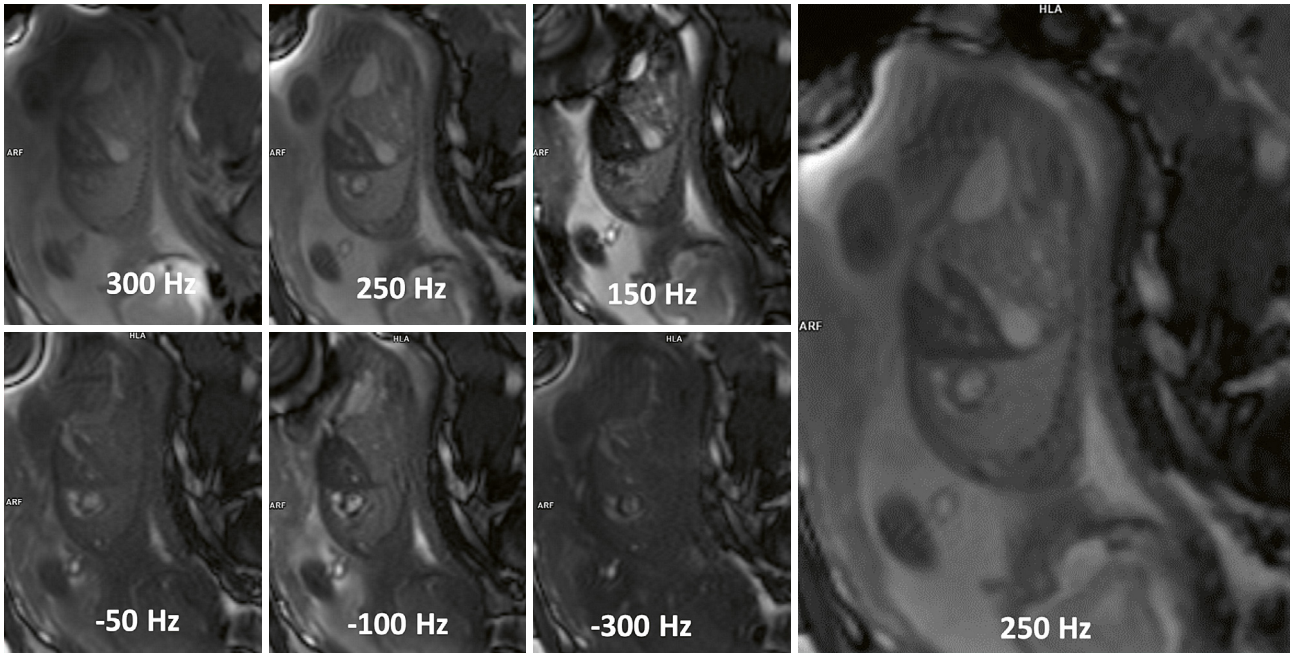

5 Single slice sagittal views of the frequency scout featuring 12 different offset frequencies (only 6 are displayed). The frequency scout is typically planned in one or a few slices around the organ of interest. The operator and/or radiologist select the "best" frequency based on their preference for contrast and/or the absence of banding artifacts around the point of interest. Subsequently, the actual T2-weighted balanced steady-state free precession sequence is acquired.

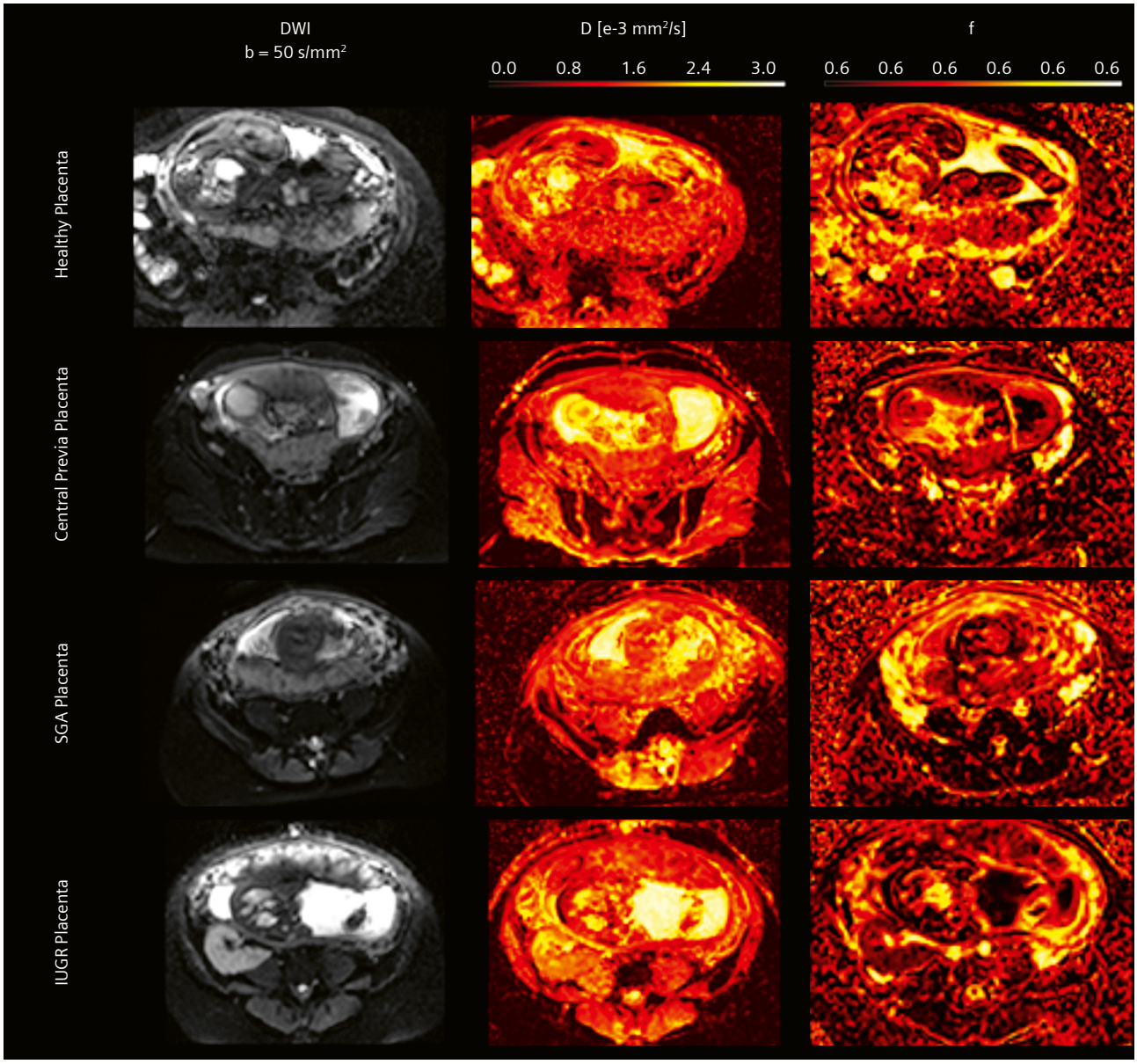

6 DWI obtained with b = 50 s/mm², and intravoxel incoherent motion f and D maps of the placenta. The normal pregnancy placenta appears with homogeneous colors in the f and D maps. In particular, the estimated value of f in fetal placenta is equal to 0.44 ± 0.06 in healthy normal placenta, and to 0.16 ± 0.04, 0.26 ± 0.04, and 0.27 ± 0.04 in central previa placenta, SGA placenta, and IUGR placenta, respectively.

However, performing cardiac imaging in fetuses presents several challenges, including unpredictable motion artifacts, the need for ECG gating, the requirement for a large field of view to avoid maternal anatomical structures, and the small size of fetal cardiovascular structures [46]. Fetal vascular and cardiac dimensions at full GA are quite small, necessitating high spatial and temporal resolution to minimize motion artifacts while maintaining diagnostic image quality. Different approaches have been developed to address these challenges [47].

One key strategy is cardiac gating, which synchronizes image acquisition with the fetal heartbeat. This ensures images are obtained during specific cardiac phases, reducing motion artifacts and improving diagnostic accuracy [48]. Cardiac gating can be achieved using methods such as metric-optimized gating (MOG), self-gating, or Doppler ultrasound gating (DUS). DUS has shown promise by synchronizing the fetal heartbeat with MRI scanning without the need for extensive post-processing [49].

Regarding the reduction of acquisition time, a new technique has emerged that uses an undersampled *k*-space acquisition and compressed-sensing (CS) reconstruction techniques. CS relies on incoherent undersampling, data sparsity, and non-linear iterative reconstruction to

Sequence	T2 HASTE	DWI IVIM	TrueFISP	T1 VIBE Dixon	TrueFISP Cine
TE (ms)	150	67	1.9	1.3	2.1
TR (ms)	1500	4500	500	6	610
TF	115	–	115	–	170
FA (°)	135	–	46	9	50
Slice thickness (mm)	2.5	3.5	3	3	3
Gap (mm)	0	0	0	0	0
AVG	1	2, 2, 2, 2, 2, 3, 3, 4, 6, 9	1	1	1
Voxel size (mm^3)	0.8 × 0.8 × 2.5	1.7 × 1.7 × 3.5	1.1 × 1.1 × 3	1.2 × 1.2 × 3	1.2 × 1.2 × 3
b-values s/mm^2	–	0, 10, 30, 50, 70, 100, 200, 400, 700, 1000 Diffusion mode: 3D diagonal	–	–	–
Acquisition time (m:s)	0:55	4:30	0:22	0:19	0:14

Table 1: 3T protocol parameters
Example protocol conducted on a 3T MAGNETOM Vida (Siemens Healthineers, Erlangen, Germany). The examination is performed using the flexible body array combined with the spine array.

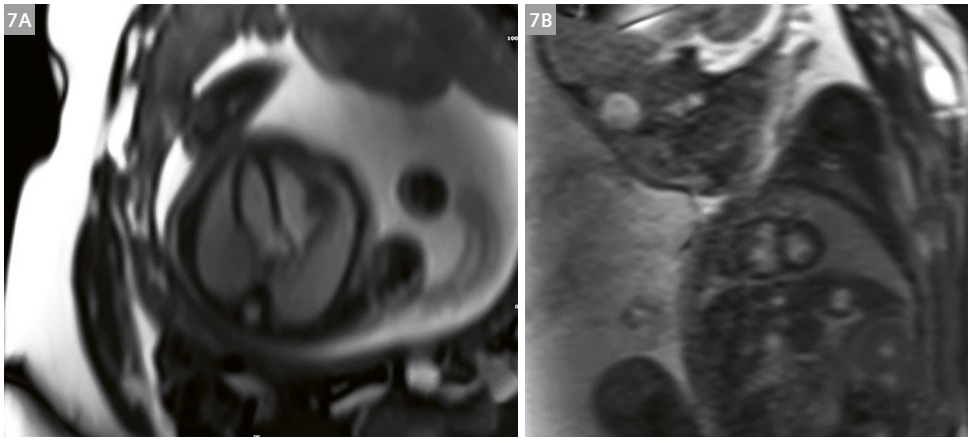

7 Cardiac views of a fetal heart: **(7A)** 4-chamber view, **(7B)** short-axis view.

obtain images much faster than traditional methods [50]. In cardiac imaging, this has enabled the acquisition of cine images in just 15–25 seconds, significantly reducing examination times and motion artifacts.

fCMR can be performed using both 1.5T and 3T MRI scanners. Before acquiring cardiac sequences, static sequences like T2-weighted turbo spin-echo or half-Fourier single-shot turbo spin-echo are used to visualize the fetal thorax in various planes. Cine TrueFISP imaging is then performed to assess cardiac and vascular anatomy, enablin g the assessment of various congenital anomalies and cardiac function parameters such as ventricular volumes and myocardial thickness [51–53] (Fig. 7).

Phase contrast MR (PC-MR) sequences are employed to measure fetal blood flow in vessels and detect shunts or valve dynamics. However, PC-MR has limitations, including limited flow information and long acquisition times [54]. On the other hand, 4D flow MRI offers a comprehensive analysis of flow patterns throughout the cardiac cycle, co-registering morphological images with flow data. Although it has advantages over fetal echocardiography, it requires careful planning due to fetal movements during image acquisition [55].

Finally, T1 and T2 mapping sequences may provide insights into oxygen delivery and consumption, which is important for understanding fetal physiology, particularly in CHD and heart failure [56].

New horizons

New avenues are opening up for fMRI. Three-dimensional (3D) reconstructions of the fetal diaphragm offer valuable insights in cases of congenital diaphragmatic hernia; they facilitate the visualization, localization, classification, and quantification of the defect. Specialized software enables segmentation of the diaphragm and the diaphragmatic defect, enabling 3D visualization across three orthogonal planes. These reconstructions can help optimize postnatal surgical planning, predict patch placement requirements, and customize patch design based on 3D-printable templates [57].

Integrating AI software into preprocessing and postprocessing MRI techniques is currently emerging as a promising approach for automating image acquisition, enhancing quality, and saving time [58]. AI expedites the labor-intensive segmentation process for various organs through automation.

Kulseng et al. [59] trained a convolutional neural network to automatically estimate placental and fetal volumes. They then compared the AI-derived values with manually calculated ones. The AI-derived values exhibited strong agreement with the manually calculated values for both placental and fetal volumes, demonstrating that AI can help reduce the processing time from over an hour to mere seconds.

AI can also be used for estimating GA. Shen et al. [60] developed an attention-guided multi-view deep learning network that was trained using a diverse dataset of 741 MR images of typical developing fetuses ranging from 19 to 39 weeks' GA. This model demonstrated the ability to predict GA with a mean absolute error of 6.7 days.

Uncontrollable, extensive, and irregular fetal movements pose challenges in fMRI acquisition. This makes the process heavily reliant on operator skill, increases magnet use and associated costs, and often results in lengthy examinations that can be burdensome for patients. In addressing this limitation, Singh et al. [61] proposed using a novel motion correction algorithm. They developed a real-time image-based motion-tracking approach based on deep learning, which directly predicts fetal head motion from acquired images. This system employs a deep regression recurrent neural network model comprising an encoder and a decoder. Integration of this technique with additional real-time components and its implementation in MRI could facilitate tracking of fetal head movements during each section acquisition, thereby assisting operators with scan orientation.

Similarly, Xu et al. [62], with the objective of reducing examination times, outlined a deep learning algorithm capable of predicting fetal position using 15 key points distributed across various body parts (such as the ankles, knees, hips, bladder, shoulders, elbows, wrists, and eyes). Additionally, other researchers [63] have demonstrated the feasibility of obtaining high-resolution 3D images of the fetal thorax and vascular structures by employing an open-source reconstruction algorithm coupled with motion correction software on 2D images. The resultant 3D images exhibit excellent spatial congruence with US measurements and noticeably enhance visualization and diagnostic quality compared to the original 2D MRI data.

Among the emerging frontiers of fMRI lies radiomics. Radiomics is an image analysis method in which a multitude of data is extracted from image data using predefined statistical operations. The objective is to unveil features that are otherwise visually imperceptible and that characterize specific tissues or forecast particular outcomes [64]. Prayer et al. [65], examining the 1.5T MRI data of 30 fetuses, showed that employing a standardized fMRI protocol enables the extraction of reproducible lung radiomics features. These features prove beneficial in complementing observed-to-expected lung volume assessments for predicting neonatal outcomes. Similarly, Song et al. [66] illustrated that MRI-based placental radiomics can effectively predict FGR. They further demonstrated that integrating radiomic features derived from MRI with fetal US indicators enhances the diagnostic accuracy of FGR.

Diffusion nuclear MRI (NMR) is constantly evolving in parallel with the development of increasingly sophisticated diffusion models to better investigate different human tissues. The work of Maiuro et al. [67, 68] represents one of the frontiers regarding the study of characteristics of highly perfused tissues, such as the placenta. In one of their works [68], a two-compartment perfusion IVIM model is used to highlight alterations in pathological placentas. In the model, f1 is the fastest perfusion fraction related to perfusion in microcapillaries and villi, and f2 is the slowest perfusion fraction related to trophoblast cell perfusion, to highlight alterations in pathological placentas.

Abbreviations

2D: two-dimensional; 3D: three-dimensional; ADC: apparent diffusion coefficient; AI: artificial intelligence; bSSFP: balanced steady-state free precession; CAIPI: controlled aliasing in parallel imaging; CHD: congenital heart disease; CS: compressed sensing; DUS: doppler ultrasound; DWI: diffusion-weighted imaging; fCMR: fetal cardiac MRI; FGR: fetal growth restriction; FLAIR: fluid attenuated inversion recovery; fMRI: fetal MRI; GA: gestational age; GRE: gradient echo; EPI: echo planar imaging; IVIM: intravoxel incoherent motion; MPRAGE: magnetization-prepared rapid gradient echo; PAS: placenta accreta spectrum; PC-MR: phase contrast MR; QSM: quantitative susceptibility mapping; SGA: small for gestational age; SPACE: sampling perfection with application-optimized contrasts using different flip angle evolution; SWI: susceptibility-weighted imaging; US: ultrasound

References

1 Triulzi F, Manganaro L, Volpe P. Fetal magnetic resonance imaging: indications, study protocols and safety. Radiol Med. 2011;116(3):337–50. English, Italian.
2 Perrone A, Savelli S, Maggi C, Di Pietro L, Di Maurizio M, Tesei J, et al. Magnetic resonance imaging versus ultrasonography in fetal pathology. Radiol Med. 2008;113(2):225–41. English, Italian.
3 Powers AM, White C, Neuberger I, Maloney JA, Stence NV, Mirsky D. Fetal MRI Neuroradiology: Indications. Clin Perinatol. 2022;49(3):573–586.
4 Masselli G, Cozzi D, Ceccanti S, Laghi F, Giancotti A, Brunelli R. Fetal body MRI for fetal and perinatal management. Clin Radiol. 2021;76(9):708.e1–708.e8.
5 Dawood Y, Buijtendijk MFJ, Shah H, Smit JA, Jacobs K, Hagoort J, et al. Imaging fetal anatomy. Semin Cell Dev Biol. 2022;131:78–92.
6 Jaimes C, Delgado J, Cunnane MB, Hedrick HL, Adzick NS, Gee MS, et al. Does 3-T fetal MRI induce adverse acoustic effects in the neonate? A preliminary study comparing postnatal auditory test performance of fetuses scanned at 1.5 and 3 T. Pediatr Radiol. 2019;49(1):37–45.
7 Manganaro L, Capuani S, Gennarini M, Miceli V, Ninkova R, Balba I, et al. Fetal MRI: what's new? A short review. Eur Radiol Exp. 2023;7(1):41.
8 Manganaro L, Bernardo S, Antonelli A, Vinci V, Saldari M, Catalano C. Fetal MRI of the central nervous system: State-of-the-art. Eur J Radiol. 2017;93:273–283.
9 Griffiths PD, Reeves MJ, Morris JE, Mason G, Russell SA, Paley MN, et al. A prospective study of fetuses with isolated ventriculomegaly investigated by antenatal sonography and in utero MR imaging. AJNR Am J Neuroradiol. 2010;31(1):106–11.
10 Parazzini C, Righini A, Doneda C, Arrigoni F, Rustico M, Lanna M, et al. Is fetal magnetic resonance imaging indicated when ultrasound isolated mild ventriculomegaly is present in pregnancies with no risk factors? Prenat Diagn. 2012;32(8):752–7.
11 Manganaro L, Antonelli A, Bernardo S, Capozza F, Petrillo R, Satta S, et al. Highlights on MRI of the fetal body. Radiol Med. 2018;123(4):271–285.
12 Ercolani G, Capuani S, Antonelli A, Camilli A, Ciulla S, Petrillo R, et al. IntraVoxel Incoherent Motion (IVIM) MRI of fetal lung and kidney: Can the perfusion fraction be a marker of normal pulmonary and renal maturation? Eur J Radiol. 2021;139:109726.
13 Antonelli A, Capuani S, Ercolani G, Dolciami M, Ciulla S, Celli V, et al. Human placental microperfusion and microstructural assessment by intra-voxel incoherent motion MRI for discriminating intrauterine growth restriction: a pilot study. J Matern Fetal Neonatal Med. 2022;35(25):9667–9674.
14 Yuan X, Yue C, Yu M, Chen P, Du P, Shao CH, et al. Fetal brain development at 25-39 weeks gestational age: A preliminary study using intravoxel incoherent motion diffusion-weighted imaging. J Magn Reson Imaging. 2019;50(3):899–909.
15 Di Trani MG, Manganaro L, Antonelli A, Guerreri M, De Feco R, Catalano C, et al. Apparent diffusion coefficient assessment of brain development in normal fetuses and ventriculomegaly. Front Phys. 2019;7, article number 160.
16 Colleran GC, Kyncl M, Garel C, Cassart M. Fetal magnetic resonance imaging at 3 Tesla - the European experience. Pediatr Radiol. 2022;52(5):959–970.
17 Prayer D, Malinger G, De Catte L, De Keersmaecker B, Gonçalves LF, Kasprian G, et al. ISUOG Practice Guidelines (updated): performance of fetal magnetic resonance imaging. Ultrasound Obstet Gynecol. 2023;61(2):278–287.
18 Weisstanner C, Gruber GM, Brugger PC, Mitter C, Diogo MC, Kasprian G, et al. Fetal MRI at 3T-ready for routine use? Br J Radiol. 2017;90(1069):20160362.
19 Chartier AL, Bouvier MJ, McPherson DR, Stepenosky JE, Taysom DA, Marks RM. The Safety of Maternal and Fetal MRI at 3 T. AJR Am J Roentgenol. 2019;213(5):1170–1173.
20 U.S. Food and Drug Administration. Criteria for significant risk investigations of magnetic resonance diagnostic devices. Center for Devices and Radiological Health, U.S. Food and Drug Administration, Rockville. 2003. Available from: ↗ https://www.fda.gov/regulatory-information/search-fda-guidance-documents/criteria-significant-risk-investigations-magnetic-resonance-diagnostic-devices-guidance-industry-and
21 Krishnamurthy U, Neelavalli J, Mody S, Yeo L, Jella PK, Saleem S, et al. MR imaging of the fetal brain at 1.5T and 3.0T field strengths: comparing specific absorption rate (SAR) and image quality. J Perinat Med. 2015;43(2):209–20.
22 Soher BJ, Dale BM, Merkle EM. A review of MR physics: 3T versus 1.5T. Magn Reson Imaging Clin N Am. 2007;15(3):277–90.
23 Merkle EM, Dale BM. Abdominal MRI at 3.0 T: the basics revisited. AJR Am J Roentgenol. 2006;186(6):1524–32.
24 Schick F. Whole-body MRI at high field: technical limits and clinical potential. Eur Radiol. 2005;15(5):946–59.
25 Victoria T, Johnson AM, Edgar JC, Zarnow DM, Vossough A, Jaramillo D. Comparison Between 1.5-T and 3-T MRI for Fetal Imaging: Is There an Advantage to Imaging With a Higher Field Strength? AJR Am J Roentgenol. 2016;206(1):195–201.
26 Bourgioti C, Zafeiropoulou K, Tzavara C, Daskalakis G, Fotopoulos S, Theodora M, et al. Comparison between 1.5-T and 3.0-T MRI for the diagnosis of placenta accreta spectrum disorders. Diagn Interv Imaging. 2022;103(9):408–417.
27 Jarvis DA, Griffiths PD. Current state of MRI of the fetal brain in utero. J Magn Reson Imaging. 2019;49(3):632–646.
28 Righini A, Arrigoni F, Izzo G, Parazzini C, Doneda C, Palumbo G. Abbreviated Turbo Spin Echo T2- and FLAIR-weighted Sequences to Complement Multiplanar HASTE images in "Quick MRI" Pediatric Brain Imaging at 3 Tesla: a child-tailored approach. ↗ MAGNETOM Flash. 2022;81(2):26–29.
29 Yadav BK, Buch S, Krishnamurthy U, Jella P, Hernandez-Andrade E, Trifan A, et al. Quantitative susceptibility mapping in the human fetus to measure blood oxygenation in the superior sagittal sinus. Eur Radiol. 2019 Apr;29(4):2017–2026.
30 Conklin J, Longo MGF, Cauley SF, Setsompop K, González RG, Schaefer PW, et al. Validation of Highly Accelerated Wave-CAIPI SWI Compared with Conventional SWI and T2*-Weighted Gradient Recalled-Echo for Routine Clinical Brain MRI at 3T. AJNR Am J Neuroradiol. 2019;40(12):2073–2080.
31 Polak D, Cauley SF, Bilgic B, Wald LL, Setsompop K. Ultrafast Multi-contrast High-resolution 3D Brain MRI: a Technical Description of Wave-CAIPI. ↗ MAGNETOM Flash. 2020;76(1):17–20.
32 Lio Goncalves Filho A, Conklin J, Rapalino O, Schaefer P, Huang S. Ultrafast Multi-Contrast High-Resolution 3D Brain MRI: Clinical Evaluation of Wave-CAIPI Acceleration in SWI, MPRAGE, FLAIR, SPACE. ↗ MAGNETOM Flash. 2020;76(1):21–27.
33 Buttin C, Dechatre N, Mauris C, Thuret A. Revisiting 3T: Pearls and Pitfalls Compared with 1.5T. ↗ MAGNETOM Flash. 2020;77(2):39–47.
34 Bieri O, Scheffler K. Fundamentals of balanced steady state free precession MRI. J Magn Reson Imaging. 2013;38(1):2–11.
35 Wansapura J, Fleck R, Crotty E, Gottliebson W. Frequency scouting for cardiac imaging with SSFP at 3 Tesla. Pediatr Radiol. 2006;36(10):1082–5.
36 Siauve N, Chalouhi GE, Deloison B, Alison M, Clement O, Ville Y, et al. Functional imaging of the human placenta with magnetic resonance. Am J Obstet Gynecol. 2015;213(4 Suppl):S103–14.
37 Bonel HM, Stolz B, Diedrichsen L, Frei K, Saar B, Tutschek B, et al. Diffusion-weighted MR imaging of the placenta in fetuses with placental insufficiency. Radiology. 2010;257(3):810–9. Erratum in: Radiology. 2011;260(1):308.

38 Han R, Huang L, Sun Z, Zhang D, Chen X, Yang X, et al. Assessment of apparent diffusion coefficient of normal fetal brain development from gestational age week 24 up to term age: a preliminary study. Fetal Diagn Ther. 2015;37(2):102–7.
39 Manganaro L, Fierro F, Tomei A, La Barbera L, Savelli S, Sollazzo P, et al. MRI and DWI: feasibility of DWI and ADC maps in the evaluation of placental changes during gestation. Prenat Diagn. 2010;30(12-13):1178–84.
40 Iima M, Le Bihan D. Clinical Intravoxel Incoherent Motion and Diffusion MR Imaging: Past, Present, and Future. Radiology. 2016;278(1):13–32.
41 Capuani S, Guerreri M, Antonelli A, Bernardo S, Porpora MG, Giancotti A, et al. Diffusion and perfusion quantified by Magnetic Resonance Imaging are markers of human placenta development in normal pregnancy. Placenta. 2017;58:33–39.
42 Slator PJ, Hutter J, McCabe L, Gomes ADS, Price AN, Panagiotaki E, et al. Placenta microstructure and microcirculation imaging with diffusion MRI. Magn Reson Med. 2018;80(2):756–766.
43 Le Bihan D, Breton E, Lallemand D, Aubin ML, Vignaud J, Laval-Jeantet M. Separation of diffusion and perfusion in intravoxel incoherent motion MR imaging. Radiology. 1988;168(2):497–505.
44 De Wilde JP, Rivers AW, Price DL. A review of the current use of magnetic resonance imaging in pregnancy and safety implications for the fetus. Prog Biophys Mol Biol. 2005;87(2-3):335–53.
45 Mamalis M, Bedei I, Schoennagel B, Kording F, Reitz JG, Wolter A, et al. The Evolution and Developing Importance of Fetal Magnetic Resonance Imaging in the Diagnosis of Congenital Cardiac Anomalies: A Systematic Review. J Clin Med. 2022;11(23):7027.
46 Haris K, Hedström E, Kording F, Bidhult S, Steding-Ehrenborg K, Ruprecht C, et al. Free-breathing fetal cardiac MRI with doppler ultrasound gating, compressed sensing, and motion compensation. J Magn Reson Imaging. 2020;51(1):260–272.
47 Roy CW, van Amerom JFP, Marini D, Seed M, Macgowan CK. Fetal Cardiac MRI: A Review of Technical Advancements. Top Magn Reson Imaging. 2019;28(5):235–244.
48 van Amerom JFP, Lloyd DFA, Price AN, Kuklisova Murgasova M, Aljabar P, Malik SJ, et al. Fetal cardiac cine imaging using highly accelerated dynamic MRI with retrospective motion correction and outlier rejection. Magn Reson Med. 2018;79(1):327–338.
49 Biko DM, Fogel MA. Fetal Cardiac MRI: Doppler US-gated Cine Imaging in Complex Congenital Heart Disease. Radiol Cardiothorac Imaging. 2023;5(1):e220314.
50 Feng L, Benkert T, Block KT, Sodickson DK, Otazo R, Chandarana H. Compressed sensing for body MRI. J Magn Reson Imaging. 2017;45(4):966–987.
51 Kording F, Yamamura J, de Sousa MT, Ruprecht C, Hedström E, Aletras AH, et al. Dynamic fetal cardiovascular magnetic resonance imaging using Doppler ultrasound gating. J Cardiovasc Magn Reson. 2018;20(1):17.

Contact

Associate Professor Lucia Manganaro, M.D.
Department of Radiological,
Oncological and Pathological Sciences
Umberto I Hospital
Sapienza University of Rome
V.le Regina Margherita, 328
00198 Roma RM
Italy
lucia.manganaro@uniroma1.it.

52 Vollbrecht TM, Hart C, Zhang S, Katemann C, Isaak A, Pieper CC, et al. Fetal Cardiac Cine MRI with Doppler US Gating in Complex Congenital Heart Disease. Radiol Cardiothorac Imaging. 2023;5(1):e220129.
53 Piek M, Ryd D, Töger J, Testud F, Hedström E, Aletras AH. Fetal 3D cardiovascular cine image acquisition using radial sampling and compressed sensing. Magn Reson Med. 2023;89(2):594–604.
54 Schoennagel BP, Yamamura J, Kording F, Fischer R, Bannas P, Adam G, et al. Fetal dynamic phase-contrast MR angiography using ultrasound gating and comparison with Doppler ultrasound measurements. Eur Radiol. 2019;29(8):4169–4176.
55 Tavares de Sousa M, Hecher K, Yamamura J, Kording F, Ruprecht C, Fehrs K, et al. Dynamic fetal cardiac magnetic resonance imaging in four-chamber view using Doppler ultrasound gating in normal fetal heart and in congenital heart disease: comparison with fetal echocardiography. Ultrasound Obstet Gynecol. 2019;53(5):669–675.
56 Udine M, Loke YH, Goudar S, Donofrio MT, Truong U, Krishnan A. The current state and potential innovation of fetal cardiac MRI. Front Pediatr. 2023;11:1219091.
57 Prayer F, Metzelder M, Krois W, Brugger PC, Gruber GM, Weber M, et al. Three-dimensional reconstruction of defects in congenital diaphragmatic hernia: a fetal MRI study. Ultrasound Obstet Gynecol. 2019;53(6):816–826.
58 Meshaka R, Gaunt T, Shelmerdine SC. Artificial intelligence applied to fetal MRI: A scoping review of current research. Br J Radiol. 2023;96(1147):20211205.
59 Kulseng CPS, Hillestad V, Eskild A, Gjesdal KI. Automatic placental and fetal volume estimation by a convolutional neural network. Placenta. 2023;134:23–29.
60 Shen L, Zheng J, Lee EH, Shpanskaya K, McKenna ES, Atluri MG, et al. Attention-guided deep learning for gestational age prediction using fetal brain MRI. Sci Rep. 2022;12(1):1408.
61 Singh A, Salehi SSM, Gholipour A. Deep Predictive Motion Tracking in Magnetic Resonance Imaging: Application to Fetal Imaging. IEEE Trans Med Imaging. 2020;39(11):3523–3534.
62 Xu J, Zhang M, Turk EA, Zhang L, Grant E, Ying K, et al. Fetal Pose Estimation in Volumetric MRI using a 3D Convolution Neural Network. Med Image Comput Comput Assist Interv. 2019;11767:403–410.
63 Lloyd DFA, Pushparajah K, Simpson JM, van Amerom JFP, van Poppel MPM, Schulz A, et al. Three-dimensional visualisation of the fetal heart using prenatal MRI with motion-corrected slice-volume registration: a prospective, single-centre cohort study. Lancet. 2019;393(10181):1619–1627.
64 Gillies RJ, Kinahan PE, Hricak H. Radiomics: Images Are More than Pictures, They Are Data. Radiology. 2016;278(2):563–77.
65 Prayer F, Watzenböck ML, Heidinger BH, Rainer J, Schmidbauer V, Prosch H, et al. Fetal MRI radiomics: non-invasive and reproducible quantification of human lung maturity. Eur Radiol. 2023;33(6):4205–4213.
66 Song F, Li R, Lin J, Lv M, Qian Z, Wang L, et al. Predicting the risk of fetal growth restriction by radiomics analysis of the placenta on T2WI: A retrospective case-control study. Placenta. 2023;134:15–22.
67 Maiuro A, Antonelli A, Manganaro L, Capuani S. Molecular diffusion and perfusion of biological water quantified by MRI for the diagnosis of pathological human placentas. Il nuovo cimento C. 2020;43:1–5.
68 Maiuro A, Ercolani G, Di Stadio F, Antonelli A, Catalano C, Manganaro L, et al. Two-Compartment Perfusion MR IVIM Model to Investigate Normal and Pathological Placental Tissue. J Magn Reson Imaging. 2024;59(3):879–891.